

## Photoexcited quantum wells: Nonlinear screening, bistability, and negative differential capacitance

R. Merlin and D. A. Kessler

*Department of Physics, The University of Michigan, Ann Arbor, Michigan 48109-1120*

(Received 21 August 1989)

The dielectric response of an electron-hole plasma confined to a slab is calculated within the Hartree approximation for electric fields perpendicular to the slab walls. The results are used to infer the capacitance behavior of photoexcited quantum-well structures under different rate conditions. Case studies show that nonlinearities in the carrier-density dependence of the energy spectrum and scattering times can lead to bistability and negative differential capacitance.

### I. INTRODUCTION

Semiconductor systems based on ultrathin ( $\approx 100 \text{ \AA}$ ) quantum wells that show strong nonlinearities in their response have received much attention in recent years.<sup>1-8</sup> This refers in particular to resonant tunneling structures<sup>1-4</sup> and to optical bistable devices<sup>5,6</sup> relying on the so-called quantum-confined Stark effect.<sup>9-15</sup> In this work, we discuss a novel kind of microscopic nonlinearity arising from two-dimensional confinement. Specifically, we consider the capacitive behavior of *photoexcited* quantum wells. Using a simple model, we find that the dielectric response of such a system exhibits two markedly different regimes which cross when the external charge and the electron-hole areal densities become equal. Focusing on particular rate conditions, we predict that nonlinearities in the response and rate equations can lead to bistability and *negative differential capacitance*. To the best of our knowledge, there are no capacitors known to exhibit these properties.<sup>16</sup>

The organization of this paper is as follows. The theoretical model is described in Sec. II. In Sec. III, we discuss the nonlinear screening properties of a quasi-two-dimensional electron-hole plasma considering its density as an independent variable. Section IV deals with particular scenarios giving unstable capacitors. In Sec. IV A we show that photoexcitation at photon energies in the vicinity of the quantum-well absorption edge can lead to capacitance bistability. The mechanism responsible for such a behavior relies on specific nonlinearities of the generation rate. Section IV B discusses an example of negative differential capacitance associated with tunneling-related instabilities. The latter requires a rapid increase in the tunneling time with increasing plasma density. A summary of our results is given in Sec. V.

### II. THEORY

Consider a quasi-two-dimensional electron-hole plasma, generated by a monochromatic photon source of flux  $S$  and frequency  $\omega_L$ , which interacts with an external electric field due to uniformly distributed charges  $\pm Q_c$  of a parallel-plate capacitor. The plasma is confined to a

semiconductor quantum well of thickness  $2L$  and effective-mass potentials  $W_{e,h}(z) = \Delta_{e,h}$  for  $|z| \leq L$  and  $W_{e,h}(z) = 0$  for  $|z| > L$  (the  $z$  axis and the field are normal to the layers, and  $\Delta_e$  and  $\Delta_h$  are the conduction- and valence-band offsets). In the Hartree approximation, the envelope functions and eigenenergies are of the form  $\Phi = \phi_j(z) \exp(i\mathbf{k} \cdot \mathbf{r})$  and  $\Lambda = \Lambda_j + \hbar^2 |\mathbf{k}|^2 / 2m_{e,h}$ , where  $j \geq 0$  is the subband index,  $\mathbf{k}$  is a wave vector parallel to the interfaces, and  $m_e, m_h$  are the electron and hole masses. The Hartree equations for the subband eigenfunctions  $\phi_j(z)$  are<sup>17</sup>

$$-(\hbar^2/2m)d^2\phi_j/dz^2 + [W(z) - 4\pi q Q_c z / A\kappa + qV_H(z) - \Lambda_j]\phi_j = 0, \quad (1)$$

where  $\phi_j = \phi_{j,e}(\phi_{j,h})$ ,  $\Lambda_j = \Lambda_{j,e}(\Lambda_{j,h})$ ,  $m = m_e(m_h)$ ,  $W = W_e(W_h)$ , and  $q = -|e|$  ( $+|e|$ ) for electron (hole) states;  $\kappa$  is the appropriate dielectric constant of the semiconductor and  $A$  is the area of the capacitor plates. The electrostatic mean-field potential  $V_H(z)$  satisfies the Poisson equation<sup>17</sup>

$$\frac{d^2 V_H}{dz^2} = \frac{4\pi|e|}{\kappa} \sum_j [n_{j,e} \phi_{j,e}^2(z) - n_{j,h} \phi_{j,h}^2(z)], \quad (2)$$

where  $n_{j,e}$  ( $n_{j,h}$ ) is the electron (hole) steady-state concentration in the  $j$ th subband (transients can be accounted for if the  $n$ 's are adiabatic variables; i.e., if the ratios  $\hbar n / n$  are negligible compared to intersubband energies). The wave functions in Eq. (2) are normalized.

The nonlinear eigenvalue problem, Eqs. (1) and (2), can be solved using standard numerical methods.<sup>17</sup> Its solutions  $\{\phi_{j,e}, \Lambda_{j,e}\}$  and  $\{\phi_{j,h}, \Lambda_{j,h}\}$  are expressed in terms of the input parameters  $Q_c$  and the populations  $\{n_{j,e}\}$  and  $\{n_{j,h}\}$ . In photoexcitation experiments, however, the subband concentrations are not determined *a priori*: the recombination, scattering, and tunneling times entering in the rate equations depend, in turn, on  $\{\phi_{j,e}, \Lambda_{j,e}\}$  and  $\{\phi_{j,h}, \Lambda_{j,h}\}$ . This leads to a system of coupled nonlinear equations which can exhibit multiple solutions for given values of  $S$ ,  $\omega_L$ , and  $Q_c$ . In the following, we present results for a neutral plasma of electrons and holes of *equal* masses confined to a slab, i.e.,  $\Delta_e = \Delta_h = \infty$ . Further-

more, it will be assumed that the only occupied levels are those associated with the ground state of the well, i.e.,  $n_{j,e} = n_{j,h} = n_0 \delta_{j0}$  (note that this condition imposes the upper bound  $n_0 < \frac{3}{4} \pi L^{-2}$  on the lowest subband concentration). This limiting case contains the necessary ingredients for nonlinear and bistable behavior while simplifying considerably the calculations.

For  $\Delta_e = \Delta_h$  and  $m_e = m_h = m_0$ , it follows from symmetry considerations that  $\phi_{j,e}(z) = \phi_{j,h}(-z)$ . Moreover, if the well is infinitely deep and states other than those of the lowest electron and hole subbands are not populated, the equations for *electrons* reduce to

$$-d^2\psi_j/dz^2 + [U(z) - E_j]\psi_j = 0, \quad (3)$$

after the transformations  $z \rightarrow Lz$ ,  $\phi_j \rightarrow L^{-1/2}\psi_j$ , and  $\Lambda_j \rightarrow \lambda E_j$  [ $\lambda \equiv \hbar^2/(2m_0^2L^2)$ ] with boundary conditions  $\psi_j(\pm 1) = 0$ . The expression for  $U(z)$  is [ $\int_{-1}^1 \psi_0^2(z) dz = 1$ ]:

$$U(z) = Qz + \sigma \int_{-z}^z [\psi_0^2(z') - \psi_0^2(-z')] dz' - 2\sigma z \int_{-1}^z [\psi_0^2(z') - \psi_0^2(-z')] dz', \quad (4)$$

where  $\sigma = 2\pi e^2 L n_0 / \kappa \lambda$  and  $Q = 4\pi |e| L Q_c / \kappa \lambda A$ . The integration constant is chosen so that  $U(0) = 0$ . Defining the total potential drop across the slab as  $2V\lambda/|e|$ , one finds

$$V = Q + 2\sigma \int_{-1}^1 z \psi_0^2(z) dz. \quad (5)$$

The inverse of the total differential capacitance of the system is  $C^{-1} = 4\pi(d - 2L)/\kappa' A + (8\pi L/\kappa A)(dV/dQ)$ , where  $d$  is the distance between the electrodes and  $\kappa'$  is the dielectric constant of the medium surrounding the slab.

Equation (5) and the self-consistent numerical solution to Eqs. (3) and (4) give  $V = V(Q, \sigma)$ . Our problem consists of simultaneously solving the latter and the appropriate rate equation. This is discussed in Sec. IV with specific examples. In the next section, we focus on  $V = V(Q, \sigma)$  alone treating  $\sigma$  as an independent parameter.

### III. NONLINEAR SCREENING

Figure 1 shows the calculated  $V(\bar{Q}, \sigma)$  together with a diagram of the system (bars on top of variables denote specific values). At low carrier densities,  $V$  varies linearly with  $\sigma$ . The slope is determined by  $\psi_0(\bar{Q}, \sigma = 0)$ . With increasing  $\sigma$ ,  $V$  crosses over (at  $\sigma \approx \bar{Q}/2$ ) to a regime showing a much weaker dependence on the concentration. The large  $\sigma$  limit shows some unusual features. Using Wentzel-Kramers-Brillouin (WKB) methods,<sup>18</sup> it can be proved<sup>19</sup> that  $V(\bar{Q}, \sigma) \propto \sigma^{-1/4}$  and that the electrostatic potential  $U$  oscillates with a period of order  $\sigma^{-1/4}$  for  $\sigma \rightarrow \infty$ . The WKB results are supported by the numerical data. Finally, the asymptotic limits of  $V(Q, \bar{\sigma})$  are  $V \propto Q$  ( $Q/2 \ll \bar{\sigma}, \partial V/\partial Q < 1$ ) and  $V = Q - 2\bar{\sigma}$  ( $Q/2 \gg \bar{\sigma}$ ). The latter reflects the fact that  $\psi_0$  approaches  $\delta(z+1)$  as  $Q \rightarrow \infty$ .

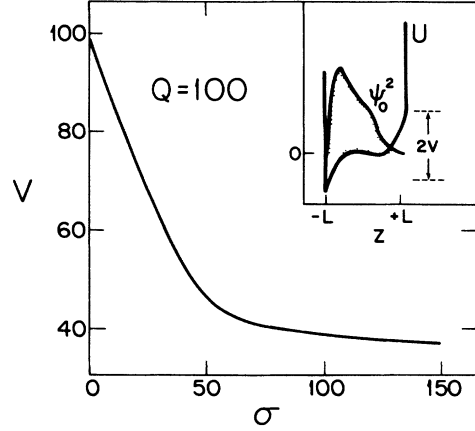


FIG. 1.  $V$  vs  $\sigma$  for  $Q = 100$ . Inset: diagram of the system showing  $\psi_0^2(z)$  and  $U(z)$  for  $Q = \sigma = 100$ .

## IV. CAPACITANCE INSTABILITIES

### A. Near-band-gap photoexcitation

Electric fields produce a red shift of the quantum-well absorption edge  $\Theta_w$ .<sup>9-14</sup> Therefore, if  $\Theta_w(Q=0)$  is slightly larger than  $\hbar\omega_L$ , the condition for creating a plasma ( $\hbar\omega_L \geq \Theta_w$ ) will eventually be met at a certain value of the field. The photogenerated plasma itself complicates this picture. Its effect on  $\Theta_w$  opposes that of  $Q$  and, provided  $S$  is sufficiently large, there will be a strong competition between the field and the plasma to define the state of the system. Under certain conditions (specified below) this competition can lead to multistable behavior.

As before, we consider a situation where the photogenerated carriers populate predominantly the lowest subband (with  $\hbar\omega_1 \approx \Theta_w$  this requires in most cases  $k_B T \ll \lambda$ ,  $T$  is the lattice temperature). In addition, the time evolution of the electron (or hole) density is assumed to obey the rate equation  $dn_0/dt = g - n_0/\tau_R$ , where  $g = (\hbar\omega_L)^{-1} 2LS\alpha$  is the photogeneration rate ( $\alpha$  is the absorption coefficient at  $\hbar\omega_L$ ) and  $\tau_R$  is the radiative recombination lifetime. Such a decay mode applies to, e.g., degenerate plasmas if field-induced tunneling can be neglected (also, note that nonradiative recombination can be easily accounted for by redefining  $\tau_R$ ).<sup>20</sup>

In terms of  $\sigma$ , the rate equation reads  $\tau_R d\sigma/dt = G - \sigma$  with  $G = (\hbar\omega_L \kappa \lambda)^{-1} 4\pi e^2 L^2 S \tau_R \alpha$ . The dependence of  $G$  on the state of the plasma involves the product  $\tau_R \alpha$ . Let  $\alpha_0$  and  $\tau_R^0$  be the absorption coefficient and the radiative lifetime at *zero field*. Within the envelope-function approximation,

$$\tau_R^{-1} \alpha \propto |\langle \phi_{0,e} | \phi_{0,h} \rangle|^2 \equiv |\langle \psi_0(z) | \psi_0(-z) \rangle|^2.$$

Accordingly, for  $\hbar\omega_L \approx \Theta_w$  and ignoring band-filling effects  $G \propto \tau_R \alpha \approx \tau_R^0 \alpha_0(\hbar\Omega)$ , where  $\hbar\Omega = [\hbar\omega_L - \Theta_w(Q, \sigma)]$ .

In the above formulation, the field and plasma lead to

rigid shifts of the generation-rate profile through the  $Q$  and  $\sigma$  dependence of  $\Theta_W$ . Noting that  $\Theta_W = \Delta_G + 2\lambda E_0$ , where  $E_0$  is the ground-state energy defined in Eq. (3) and  $\Delta_G$  is the bulk-semiconductor gap, the steady-state solutions satisfy

$$\sigma = G = [(\hbar\omega_L \kappa \lambda)^{-1} 4\pi e^2 L^2 S \tau_R^0] \times \alpha_0(\hbar\omega_L - \Delta_G - 2\lambda E_0(Q, \sigma)). \quad (6)$$

Given  $S$ ,  $\omega_L$ ,  $Q$ ,  $\alpha_0(\hbar\Omega)$ , and  $E_0(Q, \sigma)$  [Eqs. (3) and (4)], Eq. (6) can be solved for  $\sigma$ . Equation (5) is then used to obtain  $V(Q)$ . Whether or not Eq. (6) shows multiple solutions depends mainly on the form of  $\alpha_0$ . For instance, uncorrelated electron-hole pairs give  $\alpha_0 = 0$  (i.e.,  $\sigma = 0$ ) for  $\hbar\Omega \leq 0$  and a nonzero constant absorption (density) for  $\hbar\Omega \geq 0$ . Since these possibilities are incompatible the two solutions cannot coexist (note that  $E_0$  increases with increasing  $\sigma$ ).

An analysis of Eq. (6) indicates that multiplicity generally requires the existence of an absorption maximum.<sup>21</sup> Quantum wells showing sharp excitonic features should, therefore, exhibit multistable behavior.<sup>22</sup> An example is shown in Fig. 2. The calculations are for  $G = 30.0[4E_0^2 + (\Gamma/\lambda)^2]^{-1} [\hbar\omega_L = \Delta_G$  in Eq. (6)], where  $\Gamma/\lambda = 1.5$ . Corresponding parameters for a 400-Å-thick GaAs well are  $S \approx 1$  kW/cm<sup>2</sup> and  $\Gamma = 2$  meV (the maximum concentration is  $\approx 5 \times 10^{11}$  cm<sup>-2</sup>).

The origin of the multiple solutions in the example, and also in a more general case, can be understood as follows. First, we note that stability against density fluctuations requires that  $\partial(d\sigma/dt)/\partial\sigma = \partial G/\partial\sigma - 1 < 0$ . Accordingly, multistable behavior results when the latter cannot be satisfied. For this,  $\partial\alpha_0/\partial\Omega$  needs to be negative and the photon flux  $S$  needs to be large enough so as to overcome the restoring recombination term. In Fig. 2, the lower and upper branches, but not the middle branch, satisfy the stability requirement. At small  $Q$ 's, the conditions are such that the photon energy is below the  $\alpha_0$  maximum; the system is stable because  $\partial G/\partial\sigma$  is negative. With increasing  $Q$ ,  $\sigma$  increases first as the absorption profile shifts to lower energies. This continues until

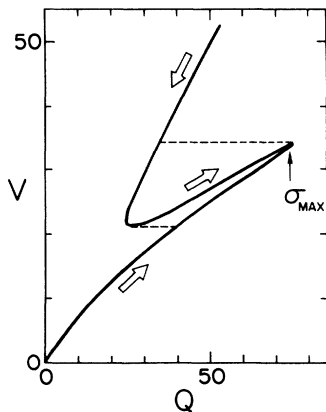


FIG. 2.  $V$  vs  $Q$  for near-band-gap photoexcitation. Parameters are given in the text.  $\sigma_{\text{MAX}}$  denotes the largest density, arrows indicate the direction of increasing  $\sigma$ , and dashed lines show the  $V$  range of bistability.

$\hbar\omega_L$  coincides with the maximum of  $\alpha_0$  (largest plasma density) and, from then on,  $\sigma$  decreases with increasing  $Q$ . The lowest branch terminates at the point where  $\partial G/\partial\sigma = 1$  (in our example, this occurs very close to the state of largest  $\sigma$ ). A further increase in  $Q$  leads to a sudden jump into the upper branch showing  $\sigma \ll V$ , i.e.,  $V \approx Q$  at large  $Q$ 's. The existence of the third, middle, branch follows from the continuity of Eq. (6). As mentioned above, this branch is unstable against  $\sigma$  fluctuations (however, note that  $dV/dQ > 0$ ) implying that the light-controlled capacitor should operate as a switch.

### B. Tunneling-induced negative differential capacitance

In this section, we consider effects due to carrier tunneling on the capacitance. Our considerations apply qualitatively to the photoexcitation behavior of a *reverse-biased* double-barrier heterostructure, such as  $\text{Al}_x\text{Ga}_{1-x}\text{As-GaAs-Al}_x\text{Ga}_{1-x}\text{As}$ , sandwiched between  $p^+$ - and  $n^+$ -doped (GaAs) layers. Referring to Sec. II, the tunneling barrier for an electron (hole) at the bottom (top) of the  $j$ th subband is given by  $[\Delta_{e,h} - \lambda(V + E_j)]$ . In what follows, we will assume that this barrier is large enough for our infinite-well model and the WKB approximation to apply, and that  $\Delta_e = \Delta_h = \Delta$ . The WKB expression for the tunneling time  $\tau_T$  is

$$\tau_T = T \exp \left\{ 2(m_B/m_0)^{1/2} \times \int [\Delta\lambda^{-1} - V - E_j - Q(z-1)]^{1/2} dz \right\}, \quad (7)$$

where  $m_B$  is the barrier effective mass and  $T$  is a constant (the integral is over the barrier layer of width  $L_B$ , i.e.,  $0 \leq z-1 \leq L_B/L$ ). The dependence of the barrier height on the plasma density follows a pattern similar to that of  $V(Q, \sigma)$  (see Fig. 1). Unlike the latter, however, the height and therefore  $\tau_T$  increase with *increasing*  $\sigma$ . In cases where the ground-state population is limited by tunneling losses, this behavior implying negative feedback can give rise to instabilities. To approach such a situation, we adopt the following scenario for the photoexcitation process: (i) the photon energy is chosen so that it resonates with a higher-lying  $j$ -subband exciton, i.e.,  $\hbar\omega_L \approx \Delta_G + 2\lambda E_j$ ; noting that, for large  $j$ 's,  $E_j$  depends only weakly on the field, the generation rate  $g$  will be treated as a constant; (ii) the photogenerated electrons and holes in the  $j$ th subband are assumed to either tunnel out of the well or decay (with time constant  $\tau_s$ ) into the corresponding lowest subbands; (iii) a single decay time  $\tau_R$  is used to characterize the radiative recombination at the ground state. For the given rate conditions, the steady-state plasma density is  $n_0 = g\tau$ , where  $\tau = (1 + \tau_s/\tau_T)^{-1}\tau_R$  or, alternatively,

$$\sigma = (\tau/\tau_R^0)G; \quad G = g2\pi e^2 L \tau_R^0 (\kappa\lambda)^{-1}. \quad (8)$$

The results in Fig. 3(a) illustrate the dependence of  $(\tau_R^0/\tau)\sigma$  on  $Q$  and  $\sigma$ . Calculation parameters are  $j = 5$ ,  $\Delta = 150\lambda$ ,  $m_B/m_0 = 1.96$ ,  $L_B/L = 0.8$ ,  $T^{-1} = 40\,000/\tau_R^0$ , and  $\tau_s = 2\tau_R^0$ . These values correspond approximately to those for electrons in a structure consisting of 160-Å-

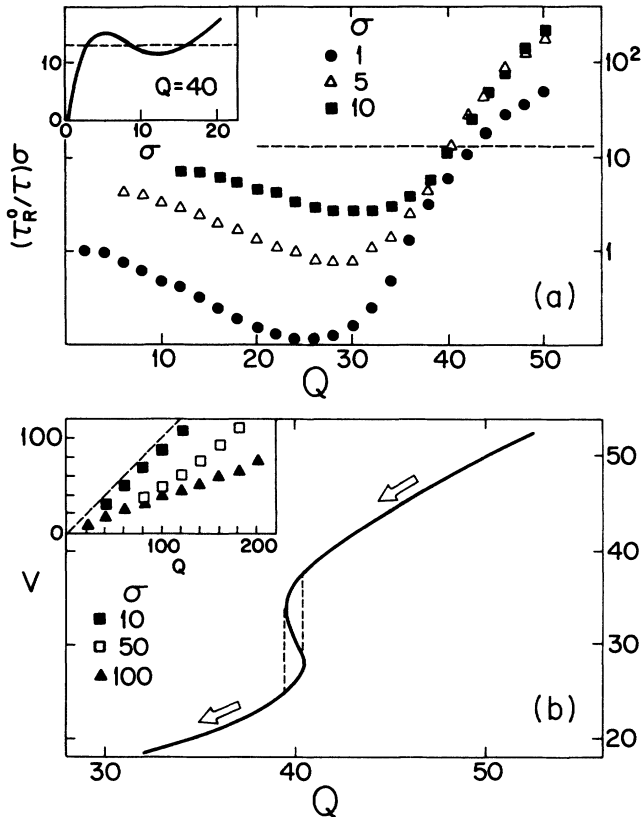


FIG. 3. Data for  $\sigma = (\tau/\tau_R^0)G$ , Eq. (8). For parameters, see text. (a)  $(\tau_R^0/\tau)\sigma$  vs  $Q$  for various densities. Inset:  $(\tau_R^0/\tau)\sigma$  as a function of  $\sigma$ . The constant (adimensional) generation rate  $G$  is indicated by dashed lines. (b)  $V(Q)$  showing negative differential capacitance. The concentration increases in the direction of the arrows. Inset:  $V$  vs  $Q$  at various densities. Dashed line is  $V = Q$ .

thick  $\text{Al}_{0.3}\text{Ga}_{0.7}\text{As}$  barriers surrounding a 400-Å-thick GaAs well (for actual values, see, e.g., Refs. 12 and 23). At low  $Q$ 's,  $\tau \approx \tau_R$  and  $(\tau_R^0/\tau)\sigma$  monotonically increases with increasing density (note that  $\partial\tau_R/\partial\sigma < 0$ ). This also applies to the tunneling-dominated high- $Q$  regime where  $\tau_T$  is nearly independent of the concentration. The crossing of curves in the intermediate range is the signature of

multistable behavior (see also the constant- $Q$  data of the inset). The solution to  $\sigma = (\tau/\tau_R^0)G$  for  $G = 13.0$  is given in Fig. 3(b) [for reference, the inset shows  $V(Q, \bar{\sigma})$ ]. As anticipated, it exhibits a  $Q$  region for which the plasma contribution to the differential capacitance is *negative* (we notice that, unlike  $Q$ , the tunneling current monotonically increases with increasing  $V$ ). The range for which  $dV/dQ < 0$  is unstable against density fluctuations, i.e.,

$$\partial(d\sigma/dt)/\partial\sigma = \partial\{\tau_R^{-1}[\sigma - (\tau/\tau_R^0)G]\}/\partial\sigma > 0.$$

We conclude with a few remarks on the validity of our approach to the case just discussed. Our model only accounts for carriers in the lowest subband and, therefore, a sufficient condition for it to apply is  $\tau_s \ll \tau_R$ . The calculations in Fig. 3 fulfill this condition. Nevertheless, we note that  $\tau_s \ll \tau_R$  is much too restrictive since the weaker  $Q$  dependence of higher states leads to a stronger cancellation of electron and hole charge distributions. These considerations indicate that the one-subband model is valid for a wider range of parameters.

## V. SUMMARY

We have described a model revealing large nonlinearities in the response of a quantum-confined plasma and presented examples showing negative differential capacitance and bistability. The cases studied correspond, in some sense, to limiting situations. More generally, one should expect instabilities resulting from a combination of those we have associated with resonant photoexcitation and tunneling. The experimental verification of our predictions holds promise for a wide range of studies in the areas of nonlinear phenomena and optoelectronic applications.

## ACKNOWLEDGMENTS

This work was supported in part by the U. S. Army Research Office under Contract No. DAAL-03-89-K-0047 and the University Research Initiative (URI) program Contract No. DAAL-03-87-K0007, and by the U. S. Department of Energy under Contract No. DE-FG02-85-ER-45189.

- <sup>1</sup>L. L. Chang, L. Esaki, and R. Tsu, Appl. Phys. Lett. **24**, 593 (1974).
- <sup>2</sup>S. Luryi, Appl. Phys. Lett. **47**, 490 (1985).
- <sup>3</sup>H. Ohnishi, T. Inata, S. Muto, N. Yokoyama, and A. Shibatomu, Appl. Phys. Lett. **49**, 1248 (1986).
- <sup>4</sup>V. J. Goldman, D. C. Tsui, and J. E. Cunningham, Phys. Rev. Lett. **58**, 1256 (1987).
- <sup>5</sup>D. A. B. Miller, D. S. Chemla, T. C. Damen, A. C. Gossard, W. Wiegmann, T. H. Wood, and C. A. Burrus, Appl. Phys. Lett. **45**, 13 (1984).
- <sup>6</sup>T. H. Wood, C. A. Burrus, D. A. B. Miller, D. S. Chemla, T. C.

Damen, A. C. Gossard, and W. Wiegmann, IEEE J. Quantum Electron. **QE-21**, 117 (1985).

- <sup>7</sup>W. H. Knox, R. L. Fork, M. C. Downer, D. A. B. Miller, D. S. Chemla, C. V. Shank, A. C. Gossard, and W. Wiegmann, Phys. Rev. Lett. **54**, 1306 (1985).
- <sup>8</sup>J. T. Remillard, H. Wang, D. G. Steel, J. Oh, J. Pamulapati, and P. K. Bhattacharya, Phys. Rev. Lett. **62**, 2861 (1989).
- <sup>9</sup>E. E. Mendez, G. Bastard, L. L. Chang, L. Esaki, H. Morkoç, and R. Fischer, Phys. Rev. B **26**, 7101 (1982).
- <sup>10</sup>D. A. B. Miller, D. S. Chemla, T. C. Damen, A. C. Gossard, W. Wiegmann, T. H. Wood, and C. A. Burrus, Phys. Rev.

- Lett. **53**, 2173 (1984).
- <sup>11</sup>D. A. B. Miller, D. S. Chemla, T. C. Damen, A. C. Gossard, W. Wiegmann, T. H. Wood, and C. A. Burrus, Phys. Rev. B **32**, 1043 (1985).
- <sup>12</sup>H.-J. Pollard, L. Schultheis, J. Kuhl, E. O. Göbel, and C. W. Tu, Phys. Rev. Lett. **55**, 2610 (1985).
- <sup>13</sup>R. T. Collins, K. v. Klitzing, and K. Ploog, Phys. Rev. B **33**, 4378 (1986).
- <sup>14</sup>I. Bar Joseph, J. M. Kuo, C. Klingshirn, G. Livescu, T. Y. Chang, D. A. B. Miller, and D. S. Chemla, Phys. Rev. Lett. **59**, 1357 (1987).
- <sup>15</sup>D. Fröhlich, R. Wille, W. Schlapp, and G. Weimann, Phys. Rev. Lett. **59**, 1748 (1987).
- <sup>16</sup>Hysteresis due to very slow traps has been observed in capacitance-voltage measurements on O-doped  $\text{Al}_x\text{Ga}_{1-x}\text{As}$  and other materials [see H. C. Casey, Jr., J. S. McCamont, H. Pandharpurkar, T. Y. Wang, and G. B. Stringfellow, Appl. Phys. Lett. **54**, 650 (1989), and references therein]. This case differs from ours in that the trap-induced bistability vanishes when the measuring frequency goes to zero.
- <sup>17</sup>See, e.g., T. Ando, A. B. Fowler, and F. Stern, Rev. Mod. Phys. **54**, 437 (1982), and references therein.
- <sup>18</sup>See, e.g., J. S. Langer, Phys. Rev. A **33**, 435 (1986).
- <sup>19</sup>D. A. Kessler and R. Merlin, Phys. Rev. B (to be published).
- <sup>20</sup>See, e.g., G. Lasher and F. Stern, Phys. Rev. **133**, 553 (1964); D. Bimberg, J. Christen, A. Werner, M. Kunst, G. Weimann, and W. Schlapp, Appl. Phys. Lett. **49**, 76 (1986).
- <sup>21</sup>Analogous considerations apply to the mechanisms discussed in Refs. 4 and 5. The maxima in the current-voltage response of resonant tunneling structures (Ref. 4) and those associated with excitons in the optical absorption (Ref. 5) are required for the observation of bistable behavior.
- <sup>22</sup>Our model, not including excitonic effects, should still provide valid results for the field-induced shifts. This is because the latter are almost completely determined by shifts of the bands as opposed to changes in the binding energy (cf. Ref. 11).
- <sup>23</sup>D. Y. Oberli, D. R. Wake, M. V. Klein, J. Klem, T. Henderson, and H. Morkoç, Phys. Rev. Lett. **59**, 696 (1987).

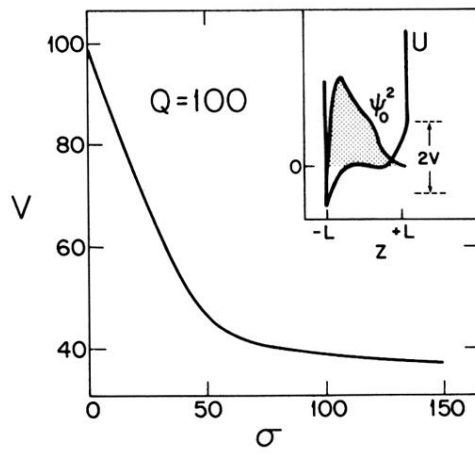


FIG. 1.  $V$  vs  $\sigma$  for  $Q=100$ . Inset: diagram of the system showing  $\psi_0^2(z)$  and  $U(z)$  for  $Q=\sigma=100$ .